Quantum Metrology Enhanced by Repetitive Quantum Error Correction

Thomas Unden, Priya Balasubramanian, Daniel Louzon, Yuval Vinkler, Martin B. Plenio, Matthew Markham, Daniel Twitchen, Alastair Stacey, Igor Lovchinsky, Alexander O. Sushkov, Mikhail D. Lukin, Alex Retzker, Boris Naydenov, Liam P. McGuinness, and Fedor Jelezko

Phys. Rev. Lett. **116**, 230502 — Published 9 June 2016

DOI: 10.1103/PhysRevLett.116.230502

Quantum metrology enhanced by repetitive quantum error correction

Thomas Unden[1], Priya Balasubramanian[1], Daniel Louzon[1,3], Yuval Vinkler[3], Martin B. Plenio[2,4], Matthew Markham[5], Daniel Twitchen[5], Alastair Stacey[6], Igor Lovchinsky[7] , Alexander O. Sushkov[7] , Mikhail D. Lukin[7], Alex Retzker[3], Boris Naydenov[1,2], Liam P. McGuinness[1], Fedor Jelezko[1,2]*

[1] Institute of Quantum Optics, Ulm University, 89081 Ulm, Germany

[2] Center for Integrated Quantum Science and Technology (IQST), Ulm University, 89081 Ulm, Germany

[3] Racah Institute of Physics, Hebrew University of Jerusalem, 91904 Jerusalem, Israel

[4] Institute for Theoretical Physics, Ulm University, 89081 Ulm, Germany

[5] Element Six, Harwell Campus, Fermi Avenue, Didcot, OX11 0QR, United Kingdom

[6] Centre for Quantum Computation and Communication Technology, School of Physics, University of Melbourne, Parkville, Melbourne VIC 3010, Australia

[7] Department of Physics, Harvard University, Cambridge, Massachusetts 02138, USA

* E-Mail: fedor.jelezko@uni-ulm.de

The accumulation of quantum phase in response to a signal is the central mechanism of quantum sensing, as such, loss of phase information presents a fundamental limitation. For this reason approaches to extend quantum coherence in the presence of noise are actively being explored. Here we experimentally protect a room-temperature hybrid spin register against environmental decoherence by performing repeated quantum error correction whilst maintaining sensitivity to signal fields. We use a long-lived nuclear spin to correct multiple phase errors on a sensitive electron spin in diamond and realize magnetic field sensing beyond the timescales set by natural decoherence. The universal extension of sensing time, robust to noise at any frequency, demonstrates the definitive advantage entangled multi-qubit systems provide for quantum sensing and offers an important complement to quantum control techniques. In particular, our work opens the door for detecting minute signals in the presence of high frequency noise, where standard protocols reach their limits.

Precise magnetic and electric field sensors constructed from qubits use the quantum phase of coherent superposition states to acquire a measurable signal. The coherence time T_2, of the qubit state therefore imposes an intrinsic limit on sensing techniques, with sensitivity scaling as $1/\sqrt{T_2}$ [1]. Following this principle, techniques to extend quantum coherence in different systems have been developed to enable the detection of weaker signals with greater precision. However, conventional methods such as environmental purification and cooling are now reaching their technical limits. Quantum control in particular has proved exceptional at extending quantum coherence by decoupling the sensor from the environment in selected frequency bandwidths [2-4]. Yet, while central to enhancing quantum metrology in noisy environments, dynamical decoupling fails in the presence of high-frequency noise with short correlation time, and is ultimately restricted by T_1 relaxation.

Recently, quantum error correction has been proposed to improve quantum metrology in the presence of noise [5-10]. Rather than driving the system faster than the typical noise frequency, as occurs in dynamical decoupling, interaction of the sensing qubit with the signal and environment remains unperturbed. Additional qubits then allow unwanted entropy introduced from the environment to be selectively extracted through quantum logic operations. By virtue of placing no restriction on the frequency spectrum of environmental noise, error correction operates when the sensor is subjected to fast noise and thus constitutes a promising alternative to state-of-the-art quantum sensing techniques. In the context of quantum information processing, quantum error correction and coherent feedback with a nuclear spin quantum register was recently demonstrated with nitrogen-vacancy (NV) centers [11-13] and several other quantum systems [14-16]. In what follows we apply quantum error correction to enhance the sensitivity of quantum metrology under ambient conditions. We show full control over the register including multiple resets of sensing qubit without perturbing the robust qubit, allowing up to two rounds of repetitive quantum error correction to be performed. We subsequently apply error correction to improve the sensor's phase coherence time in the presence of natural errors that do not affect the robust qubit, whilst also demonstrating high frequency magnetic field sensing over extended time periods.

Our experiments are based on a hybrid quantum register formed by the electronic spin of an NV center and a nearby ^{13}C nuclear spin in diamond that exhibit remarkably long coherence times even under ambient conditions [17] (Figure 1.A). Both spins can be coherently prepared with high fidelity and independently manipulated; using microwave (MW) radiation in the case of the electron $m_s = 0,\text{-}1$ states ($|0\rangle$, $|-1\rangle$), and radiofrequency (RF) radiation in the case of the nuclear $m_s = \pm ½$ states ($|\uparrow\rangle$, $|\downarrow\rangle$). Magnetic dipolar interaction between the spins further allows for quantum gates to be performed (Figure 1.B). Use of a hybrid register where a robust qubit with long T_2 time and a sensing qubit which interacts strongly with the signal (but with significantly shorter T_2 time) are simultaneously available, allows a quantum error correction protocol specific for quantum metrology to be designed. In our protocol, which we term quantum sensing with error correction (QSEC), several noisy qubits are replaced by a single noiseless qubit, thereby requiring fewer resources than conventional majority voting with three qubit code. The robust qubit, insensitive to errors, is used to actively remove errors accumulated on the sensing qubit whilst leaving interaction with the signal unperturbed. However, we note that whilst our protocol can detect and correct errors with only two qubits, it cannot correct for unwanted evolution that occurs in the register during the time between an error and its subsequent correction.

Our QSEC approach proceeds as follows. We define a code space spanned by $|+\rangle|\downarrow\rangle$ and $|-\rangle|\uparrow\rangle$ in which dynamics mediated by the signal takes place, where $|+\rangle = |0\rangle + i|-1\rangle$ and $|-\rangle = |0\rangle - i|-1\rangle$. The experiment starts with the generation of an entangled state $|+\rangle|\downarrow\rangle + |-\rangle|\uparrow\rangle$. Information about the signal field is encoded in the accumulation of a quantum phase Φ, resulting in the state $|+\rangle|\downarrow\rangle + \exp(i\Phi)|-\rangle|\uparrow\rangle$ (see Figure 2.A). An NV phase-flip error ($|+\rangle \leftrightarrow |-\rangle$) occurring on a state in the protected code space maps the system to an orthogonal error subspace spanned by the states $|+\rangle|\uparrow\rangle$ and $|-\rangle|\downarrow\rangle$. In the error subspace, the state accumulates an additional phase $|-\rangle|\downarrow\rangle + \exp(i[\Phi + \Phi_E])|+\rangle|\uparrow\rangle$, which can be interpreted as a flip of the rotation axis of the Bloch vector. Without correction of such errors, the signal encoded in the phase of the quantum register undergoes a random walk, instead of increasing linearly with

time. By using orthogonality between the code space and the error subspace, errors can be detected and corrected to bring the system back to the code space (Fig 2.A). For simplicity, we have assumed there is no time evolution between the error occurrence and the following correction step in the scheme presented in Figure 2.A. In general, the time between an error occurrence and a following correction step cannot be ignored, and phase evolution in the error subspace limits the improvement when QSEC is used (see discussion in [18] and Figure S10). For this reason it is important that the correction rate is balanced with the error rate to optimize overall performance, thereby requiring multiple error correction steps.

Experimentally we achieve phase error correction by a three step process. First, a conditional π rotation of the electron spin around the z-axis, dependent on the nuclear state is performed (CNOT gate), which maps the accumulated phase onto the nuclear spin (Decoding). After a $\pi/2$ -pulse is applied to the electron spin, an error occurrence is manifested in the state of the NV center, namely $|0\rangle$ when there was no error and $|-1\rangle$ when there was an error. Second, the sensor qubit is optically reset conditional on an error occurring, yielding $|0\rangle|\downarrow\rangle+\exp(i\Phi)|0\rangle|\uparrow\rangle$ (Reset). Finally, a second microwave pulse followed by a CNOT gate, returns the state to the code space $|+\rangle|\downarrow\rangle+\exp(i\Phi)|-\rangle|\uparrow\rangle$ (Encoding). In the case an error did not occur, the final state, $|+\rangle|\downarrow\rangle+\exp(i\Phi)|-\rangle|\uparrow\rangle$ is identical to that which would be obtained without error correction, i.e. is unaltered by error correction. A single error correction is performed in our experiments in approximately $20\mu s$, and is limited by the hyperfine interaction strength ($50kHz$) of our register.

We use this aspect of error correction, the reset of the sensor conditional on the occurrence of an error, to counter the non-unitary nature of dephasing. In particular, when the elapsed time between error and subsequent correction is much shorter than the precession period of the corresponding Bloch vector, the uncertainty of the phase due to uncompensated evolution in the error subspace is reduced and sensing can continue with negligible phase information loss. Subsequent readout of the nuclear spin, performed by a non-demolition measurement, then ideally gives the same result regardless of errors affecting the sensing qubit. In order to be

effective, each of the multiple steps of our QSEC procedure must be repetitively applied so that correction can be performed before errors destroy the phase information. First, the signal is accumulated. Second, the accumulated signal is transferred to the nuclear spin while the entropy of the sensor is retained in the electron spin. Next, the entropy is removed by resetting the electron spin. In the final step, the electron and nuclear spin are correlated again. Such a repeated quantum error correction requires precise control of interactions in the quantum register and has only been realized for trapped ions [15].

The key element for the experiments presented in this work is the identification of a robust nuclear spin located along the axis of the NV center. In this unique physical geometry the dipolar Hamiltonian between the sensing and auxiliary qubit is secular, which allows two vital processes to be realized: *i)* precise initialization and readout of the quantum register and *ii)* optical reset of the NV spin while avoiding nuclear spin dephasing. The axial requirement may be relaxed in future experiments by selecting a weakly coupled nuclear spin and employing a high external magnetic field or RF-driving of the nuclear spin during optical reset.

We first investigated the ability to initialize, coherently control and readout the register. We obtained a single-shot readout fidelity of the nuclear spin of 96%, and an initialization fidelity of the register into the $|0\rangle|\uparrow\rangle$ state beyond the detection threshold. Quantum state tomography measurements on the 2×2 sub-density matrix ρ with basis states $|0\rangle|\uparrow\rangle$ and $|-1\rangle|\downarrow\rangle$ show the controlled creation of entanglement between the electronic and the nuclear part of the register (Figure 1.C). Coherence measurements of the nuclear spin under continuous optical reset of the electron spin verified the absence of nuclear dephasing for periods much longer than the reset time. For illumination periods exceeding 20 optical resets of the electronic spin, the nuclear coherence remained at about 95% of its initial value, with no decay observable (Figure 1.D).

To implement QSEC, we applied a weak magnetic field resonant with the NV spin, and recorded the acquired phase of the hybrid sensor. This scenario provides one example where QSEC has advantages over dynamical decoupling, since when the sensing field is resonant with the qubit energy scale, decoupling is impractical due to the requirement for pulse control on timescales shorter than the signal period. Of note, relaxometry techniques have recently been developed to

exploit sensing of high frequency fields, with a precision limited by the sensor dephasing time [19, 20]. In Figure 2.A,B, we present our measurement sequence which incorporates two error correction repetitions into the sensing period, and is compared to a sequence without error correction. The acquired phase of the sensor leads to rotations on the Bloch sphere which are evidenced by coherent Rabi oscillations driven by the signal field (see fast oscillation in Figure 3.A). Without error correction, the oscillations decay on a timescale of 30 μs, limited by the dephasing time of the electron spin. After application of two rounds of error correction during the sensing period, this limit is overcome and the sensing duration is significantly extended. In addition to the fast oscillating signal, a slower coherent oscillation is observable, which is due to the hyperfine interaction within the register (see simulation in Figure 3.C and [18]). The hyperfine interaction is by nature robust and causes therefore no additional dephasing of the sensor. As the frequency is well characterized it can be distinguished from the coherent oscillations caused by the signal. We also observe the hyperfine interaction in our simulation model when no error correction is used. It appears, when gate errors (Gaussian dephasing during gate application) are taken into account and is connected to an imperfectly encoded register.

It is important to note that, due to our decoding sequence (see Figure 2.A), the accumulated signal is only converted to nuclear spin population when the electronic spin is in the $|0\rangle$ state: by application of a $\pi/2$-pulse. Consequently, our readout is designed to work only when there was no earlier error. The last error correction step therefore improves the contrast of the measurement while the intermediate correction prolongs the coherent interaction between sensor and signal.

Here, we emphasize that the corrected errors are environmental without any artificial applied noise source, and are treated naturally by our QSEC scheme. Both timing and amplitude of the errors are random, and are related to laboratory temperature and magnetic field fluctuations which act to limit the phase coherence time of the sensor. In our experiments, the signal field was switched off during QEC to allow for higher process fidelity, by using robust CNOT gates this requirement can be removed.

In addition, we demonstrate the correction of fast bit-flip errors with QSEC. Here a non-resonant signal at 100 kHz was detected using a Carr-Purcell-Meiboom-Gill (CPMG) sequence and high

frequency noise of varying strength was applied to the register to reduce the electron T_1 time from several milliseconds to as short as 60 ns [18]. As shown in supplemental Figure S7, without QSEC, the acquired signal is barely resolvable due to strong errors on the register, however when QSEC is implemented, a coherent signal with high contrast is observed despite the sensor spin experiencing multiple flips which would otherwise destroy coherence. As a result, the magnetic field sensitivity after application of QSEC could be increased by more than an order of magnitude. Furthermore, by concatenating both QSEC and CPMG sequences in this measurement, we integrate quantum error correction within a dynamical decoupling protocol to further exploit their complementarity. Indeed, in environments where low frequency noise is dominant, quantum control has proven effective at extending the sensor coherence to the T_1 limit, at which point QSEC may be employed to overcome relaxation.

To characterize the metrology improvements that were experimentally achieved in the presence of natural noise, we analyzed the data in Figure 3.A using a fitting algorithm based on Bayesian statistics [21]. By fitting the probability distribution function for the sensor decoherence rate γ, we obtain a 50% improvement in coherence time $T_2 = 1/\gamma$ when repetitive error correction is used, and accordingly a narrower linewidth which allows for improved signal discrimination (Figure 3.B). Simulations based on the system's master equation confirm this improvement of the coherence time (Figure 3.C). We also analyzed improvement in sensitivity *S*, when QSEC is used, by taking into account the contrast *C* of the measured signal according to $S \propto \frac{1}{C\sqrt{T_2}}$ [1] (Figure 3.D). We find that the improvements obtained by an increase in sensing time are offset by a 30% lower contrast when QSEC is used due to imperfect gates, which also limit the number of error correction steps that can be performed. Consequently, we do not observe an absolute improvement in sensitivity. We do however, observe that at sensing times exceeding the intrinsic T_2^* time of the sensing qubit, QSEC outperforms an uncorrected qubit for magnetic sensitivity. This is an important issue, since longer coherent interaction with the signal is required for optimized quantum sensing [22, 23], which benefits from Heisenberg scaling $S \propto \frac{1}{T}$.

By analyzing the fidelity of a single correction step we observe no limit due to nuclear spin dephasing caused by the optical NV reset (see Figure 1.D). Therefore a significantly increased performance is expected if robust gates insensitive to slow drifts of the NV center Larmor frequency are implemented.

Our results show that by using repetitive QEC, environmentally induced errors can be corrected to extend the sensing duration of quantum metrology, whilst also preserving sensitivity to signal fields. The combination of a robust and a sensitive qubit in QSEC shares a resemblance with the successful application of quantum logic for spectroscopy [24] in which a highly robust but hard to measure qubit is combined with a less robust but easy to detect qubit that reports on the quantum state of the robust qubit. In QSEC these roles are interchanged and, importantly, the role of the robust qubit in our scheme is the storage of phase information during error correction and extraction of entropy. Our demonstration of quantum error correction enhanced sensing protocol will be crucial for the rapidly growing field of diamond magnetometry, especially for NV assisted nanoscale magnetic resonance imaging and magnetic resonance spectroscopy. In these experiments high frequency noise originating from the surface is the main hurdle that has to be overcome [25]. Moreover, this technique can be extended to other quantum technologies including atomic clocks, NMR and fault-tolerant quantum computation. Robust control of several nuclear spins was demonstrated recently [12, 26] and promising (easily accessible) axial nuclear spins were identified [27]. The ability to manipulate these spins creates a promising platform for realizing more advanced QSEC codes that could tackle more complex noise models [9, 28]. The techniques demonstrated here will open a new field in quantum sensing, based on quantum error correction instead of, or in combination with dynamical decoupling and will have applications in various fields of science.

This work is supported by the EU (ERC, DIADEMS, SIQS, EQUAM), DFG (SFB/TR21 and FOR1993), DARPA, an Alexander von Humboldt Professorship and Volkswagenstiftung. We thank Michael Ferner and Manfred Bürzele for technical assistance, Paz London and Junichi Isoya for stimulating discussions.

[1] J.M. Taylor, P. Cappellaro, L. Childress, L. Jiang, D. Budker, P.R. Hemmer, A. Yacoby, R. Walsworth, M.D. Lukin, High-sensitivity diamond magnetometer with nanoscale resolution, Nat Phys, 4 (2008) 810-816.
[2] J.M. Cai, B. Naydenov, R. Pfeiffer, L.P. McGuinness, K.D. Jahnke, F. Jelezko, M.B. Plenio, A. Retzker, Robust dynamical decoupling with concatenated continuous driving, New Journal of Physics, 14 (2012) 113023.
[3] L. Childress, R. Walsworth, M. Lukin, Atom-like crystal defects: From quantum computers to biological sensors, Phys Today, 67 (2014) 38-43.
[4] G. de Lange, D. Ristè, V.V. Dobrovitski, R. Hanson, Single-Spin Magnetometry with Multipulse Sensing Sequences, Physical Review Letters, 106 (2011) 080802.
[5] E.M. Kessler, I. Lovchinsky, A.O. Sushkov, M.D. Lukin, Quantum Error Correction for Metrology, Physical Review Letters, 112 (2014) 150802.
[6] G. Arrad, Y. Vinkler, D. Aharonov, A. Retzker, Increasing sensing resolution with error correction, Phys Rev Lett, 112 (2014) 150801.
[7] W. Dür, M. Skotiniotis, F. Fröwis, B. Kraus, Improved Quantum Metrology Using Quantum Error Correction, Physical Review Letters, 112 (2014) 080801.
[8] R. Ozeri, Heisenberg limited metrology using Quantum Error-Correction Codes, arXiv:1310.3432.
[9] J. Preskill, Quantum clock synchronization and quantum error correction, arXiv:quant-ph/0010098 (2000).
[10] C. Macchiavello, S.F. Huelga, J.I. Cirac, A.K. Ekert and M.B. Plenio, Decoherence and Quantum Error Correction in Frequency Standards, in: K.e. al (Ed.) Quantum Communication, Computing and Measurement 2, Kluwer Academic/Plenum Publishers, New York, 2000.
[11] T.H. Taminiau, J. Cramer, T. van der Sar, V.V. Dobrovitski, R. Hanson, Universal control and error correction in multi-qubit spin registers in diamond, Nat Nanotechnol, 9 (2014) 171-176.
[12] G. Waldherr, Y. Wang, S. Zaiser, M. Jamali, T. Schulte-Herbruggen, H. Abe, T. Ohshima, J. Isoya, J.F. Du, P. Neumann, J. Wrachtrup, Quantum error correction in a solid-state hybrid spin register, Nature, 506 (2014) 204-207.
[13] M. Hirose, P. Cappellaro, Coherent feedback control of a single qubit in diamond, Nature, 532 (2016) 77-80.
[14] J. Chiaverini, D. Leibfried, T. Schaetz, M.D. Barrett, R.B. Blakestad, J. Britton, W.M. Itano, J.D. Jost, E. Knill, C. Langer, R. Ozeri, D.J. Wineland, Realization of quantum error correction, Nature, 432 (2004) 602-605.
[15] P. Schindler, J.T. Barreiro, T. Monz, V. Nebendahl, D. Nigg, M. Chwalla, M. Hennrich, R. Blatt, Experimental repetitive quantum error correction, Science, 332 (2011) 1059-1061.
[16] M.D. Reed, L. DiCarlo, S.E. Nigg, L. Sun, L. Frunzio, S.M. Girvin, R.J. Schoelkopf, Realization of three-qubit quantum error correction with superconducting circuits, Nature, 482 (2012) 382-385.
[17] P.C. Maurer, G. Kucsko, C. Latta, L. Jiang, N.Y. Yao, S.D. Bennett, F. Pastawski, D. Hunger, N. Chisholm, M. Markham, D.J. Twitchen, J.I. Cirac, M.D. Lukin, Room-Temperature Quantum Bit Memory Exceeding One Second, Science, 336 (2012) 1283-1286.
[18] in, See Supplemental Material at [] for details of the nondemolition measurement, corresponding simulations and correction of bit-flip error

[19] S. Kolkowitz, A. Safira, A.A. High, R.C. Devlin, S. Choi, Q.P. Unterreithmeier, D. Patterson, A.S. Zibrov, V.E. Manucharyan, H. Park, M.D. Lukin, Probing Johnson noise and ballistic transport in normal metals with a single-spin qubit, Science, 347 (2015) 1129-1132.
[20] S. Steinert, F. Ziem, L.T. Hall, A. Zappe, M. Schweikert, N. Götz, A. Aird, G. Balasubramanian, L. Hollenberg, J. Wrachtrup, Magnetic spin imaging under ambient conditions with sub-cellular resolution, Nat Commun, 4 (2013) 1607.
[21] L.C. Pardo, M. Rovira-Esteva, S. Busch, J.F. Moulin, J.L. Tamarit, Fitting in a complex χ^2 landscape using an optimized hypersurface sampling, Physical Review E, 84 (2011) 046711.
[22] C. Bonato, M.S. Blok, H.T. Dinani, D.W. Berry, M.L. Markham, D.J. Twitchen, HansonR, Optimized quantum sensing with a single electron spin using real-time adaptive measurements, Nat Nano, advance online publication (2015).
[23] G. Waldherr, J. Beck, P. Neumann, R.S. Said, M. Nitsche, M.L. Markham, D.J. Twitchen, J. Twamley, F. Jelezko, J. Wrachtrup, High-dynamic-range magnetometry with a single nuclear spin in diamond, Nat Nano, 7 (2012) 105-108.
[24] P.O. Schmidt, T. Rosenband, C. Langer, W.M. Itano, J.C. Bergquist, D.J. Wineland, Spectroscopy using quantum logic, Science, 309 (2005) 749-752.
[25] Y. Romach, C. Müller, T. Unden, L.J. Rogers, T. Isoda, K.M. Itoh, M. Markham, A. Stacey, J. Meijer, S. Pezzagna, B. Naydenov, L.P. McGuinness, N. Bar-Gill, F. Jelezko, Spectroscopy of Surface-Induced Noise Using Shallow Spins in Diamond, Physical Review Letters, 114 (2015) 017601.
[26] A. Dreau, P. Spinicelli, J.R. Maze, J.F. Roch, V. Jacques, Single-shot readout of multiple nuclear spin qubits in diamond under ambient conditions, Phys Rev Lett, 110 (2013) 060502.
[27] A.P. Nizovtsev, S.Y. Kilin, A.L. Pushkarchuk, V.A. Pushkarchuk, F. Jelezko, Theoretical study of hyperfine interactions and optically detected magnetic resonance spectra by simulation of the C 291 [NV] - H 172 diamond cluster hosting nitrogen-vacancy center, New J Phys, 16 (2014) 083014.
[28] D.A. Herrera-Martí, T. Gefen, D. Aharonov, N. Katz, A. Retzker, Quantum Error-Correction-Enhanced Magnetometer Overcoming the Limit Imposed by Relaxation, Physical Review Letters, 115 (2015) 200501.
[29] P. Neumann, J. Beck, M. Steiner, F. Rempp, H. Fedder, P.R. Hemmer, J. Wrachtrup, F. Jelezko, Single-Shot Readout of a Single Nuclear Spin, Science, 329 (2010) 542-544.

Figure 1.

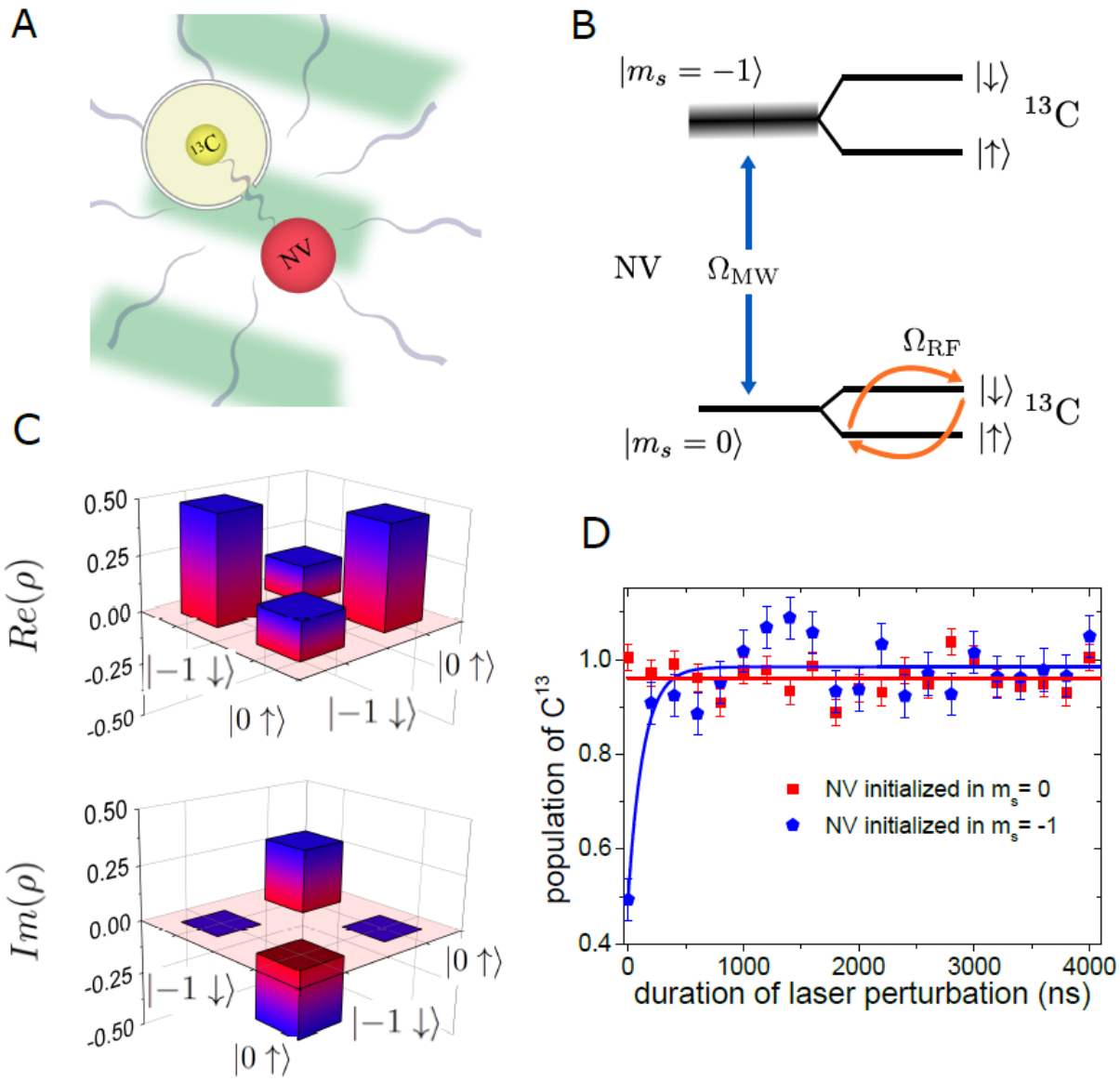

Fig. 1. Quantum system of interest and its fundamental properties. **A.** Quantum register formed by a NV and a near-axial ^{13}C nucleus (auxiliary qubit) in the diamond lattice. **B**. Energy level structure of the quantum register, showing the ground state spin manifold $|0\rangle$, $|-1\rangle$ of the NV center and the spin manifold $|\uparrow\rangle$, $|\downarrow\rangle$ of the ^{13}C spin. The NV-spin transitions are driven by a resonant microwave signal Ω_{MW} and the nuclear spin is driven by a radiofrequency signal Ω_{RF}. To resolve the energy degeneracy of the NV spin states $|\pm 1\rangle$ and to define the NV qubit corresponding to the states $|0\rangle$ and $|-1\rangle$, an external magnetic field of about 340 G was applied. The magnetic field is aligned to the symmetry axis of the NV center. The coupling between NV center and nuclear spin is given by the hyperfine interaction, which in our case shows only a

parallel component of 50 kHz (note that other non-axial nuclear spins can also be employed as robust qubits). The depicted broadening of the $|-1\rangle$ energy level corresponds to fluctuations of the NV Larmor frequency induced by the environment. **C**. Quantum state tomography performed in the subspace defined by the basis states $|0\rangle|\uparrow\rangle$ and $|-1\rangle|\downarrow\rangle$. We estimate a fidelity of 80% to initialize the system to the state $|0\rangle|\uparrow\rangle+i|-1\rangle|\downarrow\rangle$, when the remaining entries of the full 6×6 density matrix are neglected. **D**. Nuclear coherence under optical excitation of the NV center as measured by free induction decay of the nuclear spin. During the nuclear free evolution time, continuous optical excitation of NV is performed. The NV was initially prepared in either the $|0\rangle$ or the $|-1\rangle$ state. After free evolution of the nuclear spin, a $\pi/2$ pulse conditional on the electronic spin state $|0\rangle$ was applied to the nuclear spin to convert the nuclear coherence to population difference and a projective measurement was subsequently performed.

Figure 2.

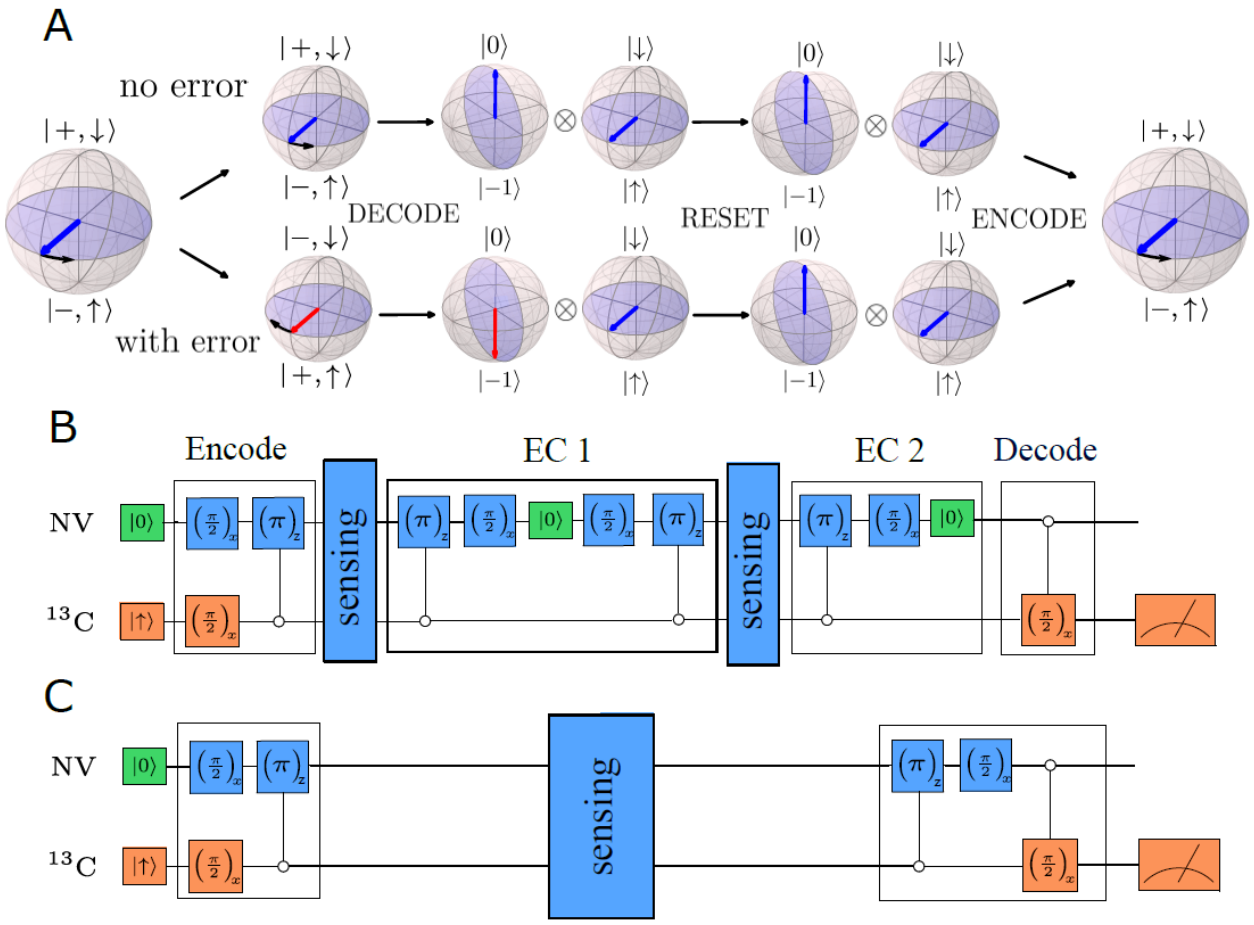

Fig. 2. Temporal evolution of the hybrid register and the implemented quantum sensing with error correction (QSEC) scheme. **A**. QSEC protocol in Bloch sphere representation, showing decoding (disentanglement), reset of the NV spin, and encoding. The error in this scheme is a single phase-flip of the NV. No time evolution between error and correction steps is assumed. The presented scheme is the basic correction step, which is applied repetitively (up to two times). The phase of the initial state corresponds to the signal. **B**. Measurement sequence used in the experiment when QSEC is used. First the electron and the nuclear spins were initialized via a laser pulse and single shot measurement. To encode the system in the state $|+\downarrow\rangle+|-\uparrow\rangle$, local operations are applied with microwave and radiofrequency pulses. For entanglement creation with a controlled-not gate ($CNOT_z$), the parallel hyperfine interaction between NV and ^{13}C is used. All control pulses are performed on resonance to a single NV transition corresponding to a certain nuclear spin state. After encoding, a microwave signal with variable time duration is applied, resonant with the electronic part of the register and coherent signal accumulation occurs.

During the first error correction step, entanglement between the NV and nuclear spins is removed by a CNOT gate, then a reset of the NV is performed and finally the entangled state is prepared for further sensing. After the second period of coherent interaction with the microwave signal, a further error correction step is applied. To readout the phase of the state $\left|+\downarrow\right\rangle+e^{i\phi}\left|-\uparrow\right\rangle$, it is mapped onto the local phase of the nuclear spin and readout after a conditional $\pi/2$ pulse by performing a non-demolition measurement. **C**. The measurement sequence used in the experiment when no error correction is used. The measurement sequence follows that shown in B, but without the intermediate and last error correction steps.

Figure 3.

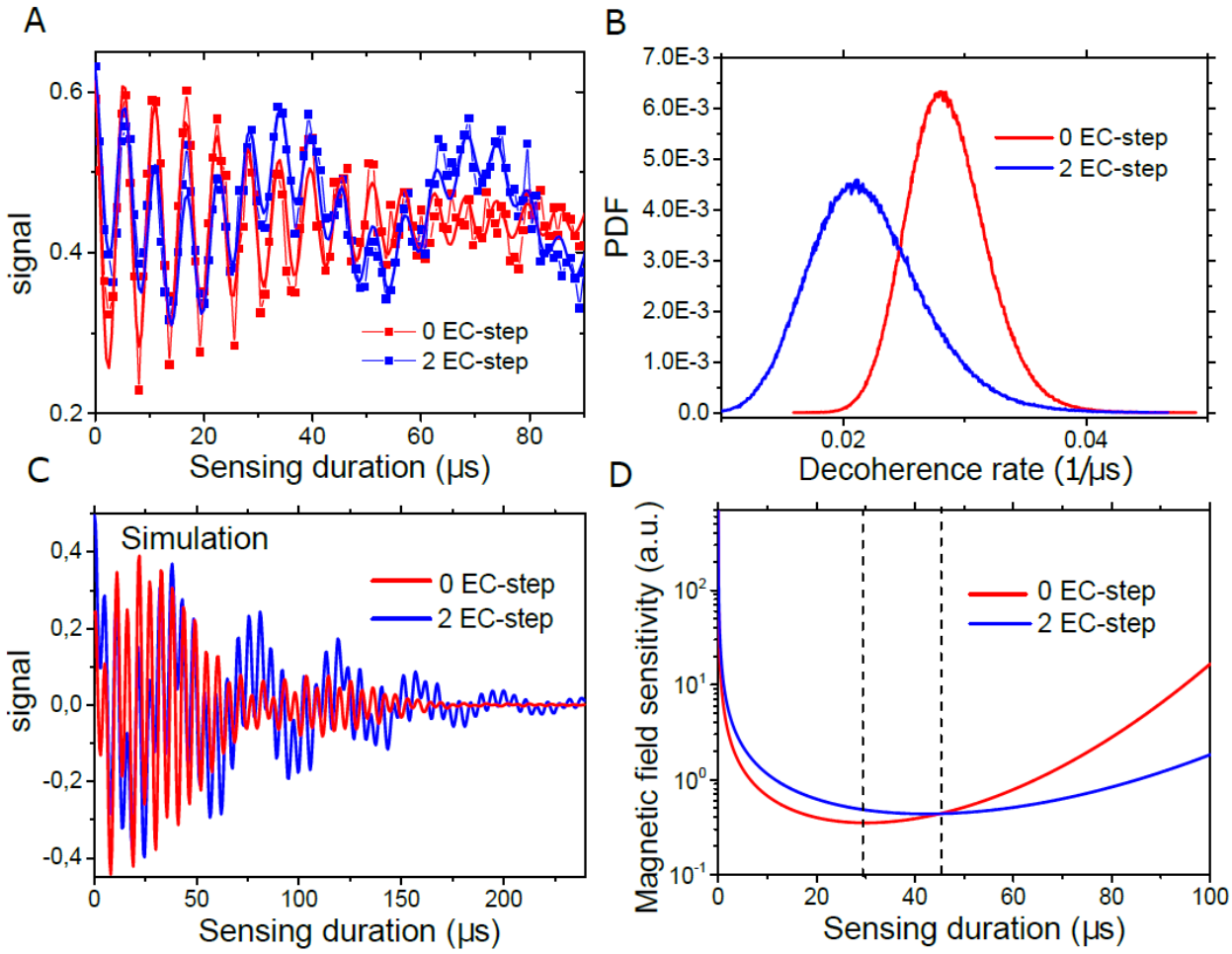

Fig. 3. Performance of QSEC against natural noise and sensitivity analysis. **A**. NV Rabi oscillations based on the sequences in Figure 2.B and in 2.C comparing the signal when no EC is used and when two EC steps are performed. In the case where EC was used, a slower oscillation appears. This oscillation corresponds to half of the hyperfine interaction strength ($50\,kHz$) and is connected to the unitary evolution mediated by the hyperfine coupling within the register itself. For both experiments, the same overall measurement time was used. The solid lines correspond to fits. In the case of no EC, we used $f(x) = A \cdot e^{-\gamma \cdot x} \cdot \cos(\omega \cdot x + \varphi) + c$ and in the case with EC $f(x) = A_1 e^{-\Gamma \cdot x} \cos(\omega_1 \cdot x + \varphi_1) + A_2 e^{-\gamma \cdot x} \cdot \cos(\omega_2 \cdot x + \varphi_2) + c$ to fit the measurement data. **B**. Probability distribution function (PDF) of the fit parameter γ based on Bayesian estimation. The fit parameter γ corresponds to the rate of the observed decoherence with (blue) and without (red) QSEC. **C**. Simulation of the measurement data, based on a master equation which takes slow fluctuation of the NV Larmor frequency into account. More information about the simulation model can be found in [18]. **D.** Magnetic sensitivity of the

sensor as a function of sensing time with and without QSEC. The shown sensitivities are calculated based on the estimated parameter describing the measurement data shown in Figure 3.A. The dashed lines indicate the sensing duration which gives the best achievable sensitivity. The sensing duration is the time of sensing, neglecting the time needed for initialization, readout and error correction.